

Measurement of a small vertical emittance with a laser wire beam profile monitor

Hiroshi Sakai,* Yousuke Honda, and Noboru Sasao[†]

Department of Physics, Kyoto University, Kyoto 606-8502, Japan

Sakae Araki, Hitoshi Hayano, Yasuo Higashi, Kiyoshi Kubo, Toshiyuki Okugi, Takashi Taniguchi,
Nobuhiro Terunuma, and Junji Urakawa

High Energy Accelerator Research Organization (KEK), Ibaraki 305-0801, Japan

Mikio Takano[‡]

Department of Physics, Toho University, Funabashi, Chiba 274-8510, Japan

(Received 31 March 2002; revised manuscript received 2 December 2002; published 17 December 2002)

We describe in this paper a measurement of vertical emittance in the Accelerator Test Facility (ATF) damping ring at KEK with a laser wire beam profile monitor. This monitor is based on the Compton scattering process of electrons with a laser light target which is produced by injecting a cw laser beam into a Fabry-Perot optical cavity. We installed the monitor at a straight section of the damping ring and measured the vertical emittance with three different ring conditions. In all cases, the ATF ring was operated at 1.28 GeV in a single bunch mode. When the ring was tuned for ultralow emittance, the vertical emittance of $\varepsilon_y = (1.18 \pm 0.08) \times 10^{-11}$ mrad was achieved. This shows that the ATF damping ring has realized its target value also vertically.

DOI: 10.1103/PhysRevSTAB.5.122801

PACS numbers: 07.60.Ly, 41.75.Ht, 42.60.Da

I. INTRODUCTION

In high energy physics, one of the major future projects is to build a TeV-region linear collider; it is hoped to allow us precision tests of the standard model, detailed studies of yet-to-be-discovered Higgs particles, search for new particles such as those predicted by supersymmetric theories, etc. The Accelerator Test Facility (ATF) at KEK was built to develop necessary techniques for such a linear collider. In particular, one of the main tasks is to establish production and manipulation techniques for an ultralow emittance beam. The ATF consists of three parts: a 1.28 GeV S-band electron linac, a damping ring, and an extraction line [1]. The beam size is reduced to $<100 \mu\text{m}$ horizontally and $<10 \mu\text{m}$ vertically in the damping ring. As to the emittance (at zero current), 1.1×10^{-9} mrad is the designed value for the horizontal and 1.1×10^{-11} mrad is the target value for the vertical.

Presently, there are three ways to measure the beam sizes at the ATF: tungsten wire scanners, a synchrotron radiation (SR) beam profile monitor, and a laser wire monitor. The wire scanners, placed at the extraction line, can measure extracted beam sizes. In fact, they measured the horizontal beam sizes successfully and confirmed that the designed value was achieved for the horizontal emittance [2]. As for the vertical emittance, however, much more precise measurements are required because its value is expected to be only $\sim 1/100$ of the horizontal one. For the wire scanners, one cannot neglect effects such as beam position jitter due to the kicker magnet fluctuation, residual dispersion, and coupling between the horizontal and vertical emittances caused by nonlinearity in the magnetic fields, all characteristic of

the extraction line. Accordingly, much more careful studies are needed before reliable values are extracted for the vertical emittance. The SR interferometer, installed in the ring, can provide fast and convenient beam size measurements. Its results are used routinely to tune the ATF damping ring parameters. However, the vertical beam size measurement is a difficult task for this type of monitor, too. This is due in part to poor SR intensity and some instrumental uncertainty [3], and no reliable measurements on the vertical emittance have been made up to now. In view of the situation above, the laser wire monitor has been developed; its main goal is to directly measure the vertical beam size in the damping ring.

A brief description of the laser wire monitor [4] and a preliminary result of the beam size measurement [5] were already reported. In our previous measurement, however, due to inadequacy of the laser wire intensity, the statistical power and thus the signal-to-noise ratio were rather poor, and it was not possible to measure, for example, current dependence of the beam size. Thus, after the measurement, various efforts were made to improve the system; these include increase in the cavity's effective power, modification of a laser power modulation scheme, etc. A full account of the upgraded laser wire monitor has already been given elsewhere [6]. In this paper, we report in detail on a measurement of vertical emittance in the ring with the upgraded monitor.

The paper is organized as follows. Section II is devoted to describe our experimental setup. Data analysis and its results are presented, respectively, in Secs. III and IV. The conclusion of the present study is given in Sec. V.

II. EXPERIMENTAL SETUP

The experimental setup, shown in Fig. 1, consists of two main components: a laser wire system and a photon detector system. An electron beam coming from the right in the figure interacts with a laser light via the Compton scattering process and emits photons in a narrow cone in the forward direction. These photons are detected by the photon detector made with a pure CsI scintillation counter placed 12.8 m downstream of the cavity. The detector energy scale was calibrated with ^{22}Na (0.511 MeV, 1.275 MeV) and ^{137}Cs (0.662 MeV) gamma sources, and its stability during the experiment was monitored using a light-emitting diode. In order to enhance the signal-to-noise ratio, a 100-mm-thick lead block collimator with a 5-mm-diameter bore at the center is placed in front of the detector. Figure 2 shows our expected energy spectrum of the Compton scattered photons. The solid line represents the spectrum without detector response, in which the highest energy, 28.6 MeV, is determined by kinematics while the lowest value is set by the collimator size. The shaded histogram shows the spectrum smeared by detector energy resolution. All equipment of the laser wire system is mounted on a movable table. Count rates of scattered photons are measured as a function of laser wire vertical positions. The vertical emittance is deduced from this profile, together with other measured quantities such as β functions and the laser beam waist. It is appropriate here to comment on the speed of this monitor. As will be shown below, it takes about an hour to make one complete measurement. On the other hand, the damping time of the vertical emittance is calculated to be about 29 msec

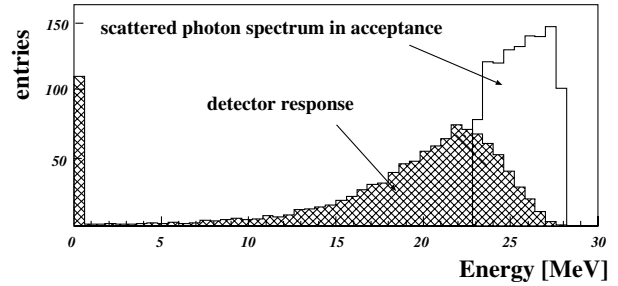


FIG. 2. Expected energy spectrum. The solid histogram shows the scattered photon energy spectrum passing through the collimator while the hatched histogram represents the spectrum smeared by detector resolution.

[7]. Thus this monitor essentially measures the equilibrium emittance.

Below we briefly describe the laser wire system, mainly focusing on the points upgraded from the previous measurement. The details can be found in [6].

A. Laser wire

In a damping ring, a vertical beam size is reduced within $10\ \mu\text{m}$. In order to measure such a small size, a thin and intense laser beam is needed. This is realized by injecting a cw laser beam (100 mW, $\lambda = 532\ \text{nm}$) into a Fabry-Perot optical cavity. Two parameters are important from the viewpoint of the emittance measurement: a beam waist (w_0) which represents the thinness of the laser beam in the cavity, and a cavity's power gain (S_{res}). The beam waist and the gain were measured before

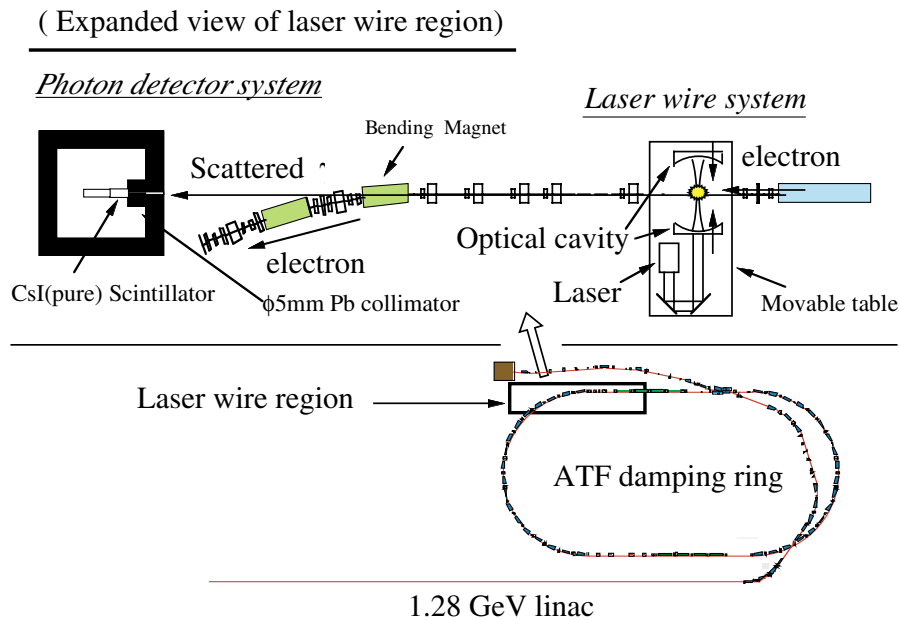


FIG. 1. (Color) Experimental setup of the emittance measurement. The laser wire monitor is installed at the north straight section of the ATF damping ring.

and after the emittance measurement and were found to be consistent with each other. The resultant values are $w_0 = 14.5 \pm 0.5 \mu\text{m}$ and $S_{\text{res}} = 220 \pm 20$. Taking into account all other factors, the effective power inside the cavity is estimated to be $11 \pm 1 \text{ W}$ [6]. This value is about 5 times larger than the previous one [5]. The improvement came from an increase in the laser original power ($\times 2$), improvement in the cavity gain by employing a mirror with higher reflectivity ($\times 2$), and improvement in matching efficiency ($\times 1.3$).

B. Laser modulation

There exists rather severe photon backgrounds [8] in this experiment, and they must be subtracted statistically to single out the genuine Compton signal. The background counts can be obtained by laser-off data. This process was done manually in the previous experiment. However, in the present measurement, this was done by modulating the laser power inside the cavity. Figure 3 shows a transmitted laser intensity signal from the cavity together with other relevant signals. We note that the transmission signal is actually obtained by a photodiode placed behind the cavity, and that it is proportional to the cavity's effective beam power. The bottom signal is a 1 kHz square wave signal (basic clock), and the middle one, obtained by integrating the basic clock, is a modulation signal fed into a piezoactuator, which controls the cavity length. As seen in Fig. 3, the modulation amplitude is large enough to cover one entire resonance peak. The count rate of the Compton signal must be proportional to the laser effective power.

C. Readout electronics and logics

An output from the CsI photon detector was first amplified and then divided into four identical signals. They were then discriminated by discriminators with different threshold levels corresponding to 5, 15, 25, and 35 MeV. The output from each discriminator was fanned out into five signals, which were in turn fed into different scalars. We prepared five scalars, each of which had (at least) four

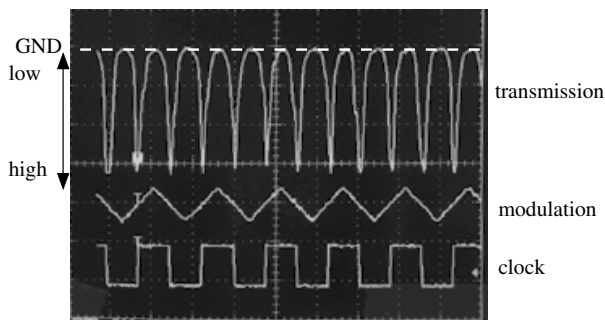


FIG. 3. Laser modulation. The transmitted laser intensity (top), the modulation signal fed into the piezoactuator (middle), and the basic clock signal (bottom).

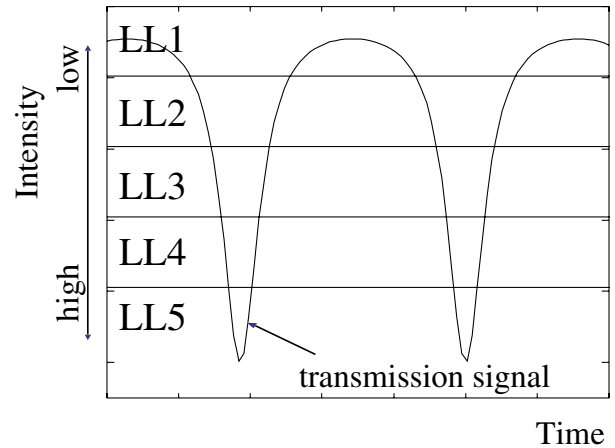


FIG. 4. (Color) Schematics of the transmitted laser signals and the MLC levels.

inputs accepting the detector signal of different deposit energy ranges. The scalars had a run/inhibit mode; this mode was controlled by transmitted laser intensity which was classified into five intensity levels by a module called a multilevel comparator (MLC). Figure 4 shows comparator levels set for the transmission signal. Each scaler counted only when the laser intensity exceeded the corresponding comparator level. One scaler, however, always read counts irrespective of the laser intensity. In the off-line analysis, we classified scaler counts according to the five laser intensity levels (LL1–LL5) and four photon energy ranges.

The data from scalars were read by a local computer via a CAMAC system every 1 s. Information from photodiode signals, beam position monitors, electron current, and vacuum pressure was also recorded. In particular, stability of the incident laser beam as well as the transmitted one from the cavity were recorded by an analog-to-digital converter during the entire experiment. The incident beam was found to be stable within 0.5%, and the transmitted intensities corresponding to five different levels of LL1–LL5 were within a few percent of their respective averages.

D. Data taking procedure

First we searched for Compton signals by scanning the vertically movable table on which the system was installed. Having found the Compton signals, we then scanned horizontally the position of the detector and a collimator to maximize the signal rate. Then data were taken following the steps listed.

- (1) Set the movable table at one vertical position.
- (2) Store an electron beam in the damping ring.
- (3) Take data every second for 10–15 min.
- (4) Repeat the procedures (1)–(3). The procedures from (1)–(3) were defined as a single run. These runs were continued until the laser wire covered an entire electron beam profile.

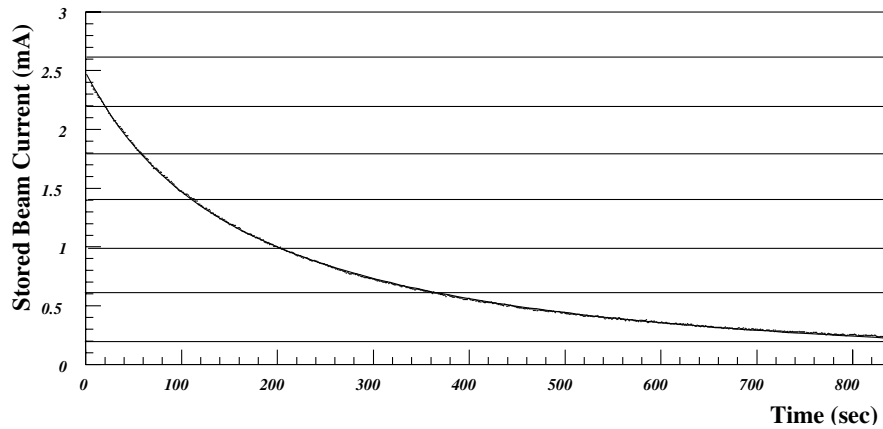


FIG. 5. Electron beam current versus time for one fill. The horizontal lines show the current intervals used to classify scalar counts.

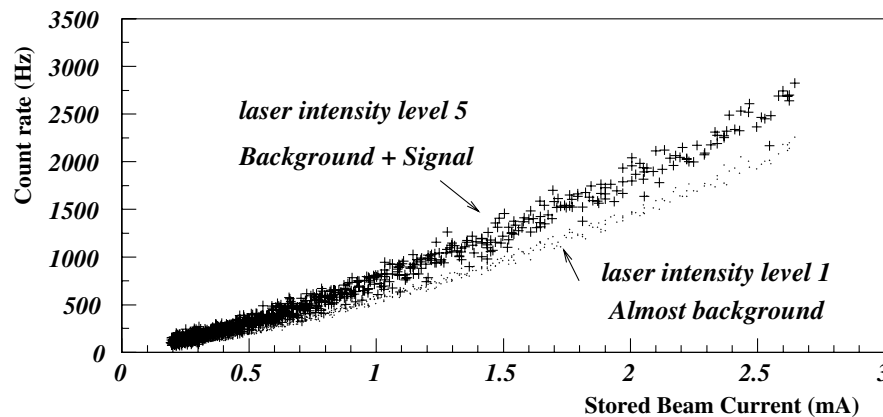


FIG. 6. Raw count rate versus electron beam current. The cross points show laser-on data (laser intensity level 5) while the dotted points show laser-off data (laser intensity level 1).

Figure 5 shows a typical example of the electron beam current (I_e) in the damping ring in one run. The horizontal lines in the figure show the current intervals used to classify scalar counts and will be explained in detail below. In order to illustrate background-to-signal ratio in our experiment, examples of raw counts, corresponding to an energy range of 15–25 MeV and taken when the laser wire was right on the electron beam, are plotted in Fig. 6 as a function of the electron beam current. The cross points represent the laser-on (laser intensity level 5) data while the dotted points show the laser-off (level 1) data. Background is non-negligible but the difference is clear.

E. Beam tuning and data

We measured the vertical emittance 3 times with different ring conditions. In all cases, the ATF ring was operated at 1.28 GeV in a single bunch mode. Procedures of beam tuning, done prior to the emittance measurement, are described briefly below.

First, closed orbit distortion and vertical momentum dispersion were reduced as much as possible. Then, coupling between horizontal and vertical betatron oscillations was minimized. This process, called “skew correction,” was a key to the production of an ultralow emittance beam [9]. The measurement dates and tuning conditions are listed below.

(1) The skew correction was carefully performed to make the vertical emittance as small as possible (2000/12/5).

(2) We skipped the skew correction on purpose, expecting large emittance due to the x - y betatron coupling. This measurement was performed to confirm the x - y coupling effect and to obtain the response of the laser wire measurement to the emittance growth (2000/12/7).

(3) The purpose of the 3rd measurement was to confirm the 1st one. However, as it will be described, the conditions of the ring, especially its β function and tune ν , turned out to be somewhat different from those in 1 (2000/12/14).

During the beam tuning process, we also measured important ring parameters such as the tune ν , β functions, etc. The procedures together with their results are described in Sec. IIIC.

III. DATA ANALYSIS

A. Overview

Before we go into the data analysis, we present the relations between the beam emittance ε_y and various measured quantities. The observed (σ_{obs}) and real (σ_y) vertical electron beam sizes are related by

$$\sigma_y = \sqrt{\sigma_{\text{obs}}^2 - \left(\frac{w_0}{2}\right)^2}, \quad (1)$$

where w_0 is the laser wire beam waist, and suffix y denotes the vertical direction. We note that both laser and electron beam profiles are assumed to be Gaussian (the normal distribution), and that w_0 corresponds to 2σ . With σ_y being measured, the emittance ε_y is given by

$$\beta_y \varepsilon_y = (\sigma_y)^2 - \left(\eta_y \frac{\sigma_p}{p}\right)^2, \quad (2)$$

where β_y and η_y are, respectively, the ring's β function and momentum dispersion function in the y direction at the laser wire position, and σ_p/p is the fractional momentum spread. The term $\eta_y(\sigma_p/p)$ can be neglected in the present experiment as will be shown later. Thus our main task is to determine three quantities: σ_{obs} , β_y , and

w_0 . Below we describe the data analysis procedure in detail.

B. Measurement of the vertical beam size

1. Signal count rates

As we explained in Sec. IIC, the number of scattered photons was counted by scalars. Scalar counts were collected simultaneously with the laser intensity level, scattered photon energy, current of the electron beam, and position of the movable table. Scalar count classification is summarized in Table I. We took the following steps to calculate the signal count rates normalized to the electron current.

(1) First we summed up each scalar count every 0.4 mA interval from 0.2 to 3.0 mA. See the horizontal lines in Fig. 5. Then we converted them to count rates (Hz).

(2) Next we plotted the count rates as a function of the laser intensity level (LL1–LL5). Figure 7 shows two examples of the plots. The data in Fig. 7, taken on (2000/12/05), corresponded to the energy range of 15–25 MeV and the electron current of 0.2–0.6 mA. The left figure shows the data in the case of the laser wire on the electron beam while the right figure off the beam. Clear linear increase of the count rate is seen only on the left. The solid lines in Fig. 7 show the results of a linear fit. These straight lines were extrapolated to the point corresponding to the laser wire maximum intensity, i.e., the cavity's maximum energy realized at the peak shown in

TABLE I. Classification of the scaler counts.

Category	Divisions	Intervals
Energy of scattered photons (MeV)	4	5–15, 15–25, 25–35, 35–
Electron current (mA)	7	0.4 interval from 0.2 to 3.0
Laser intensity (arb. units)	5	LL1, LL2, LL3, LL4, LL5
Laser wire positions (μm)	20–21	

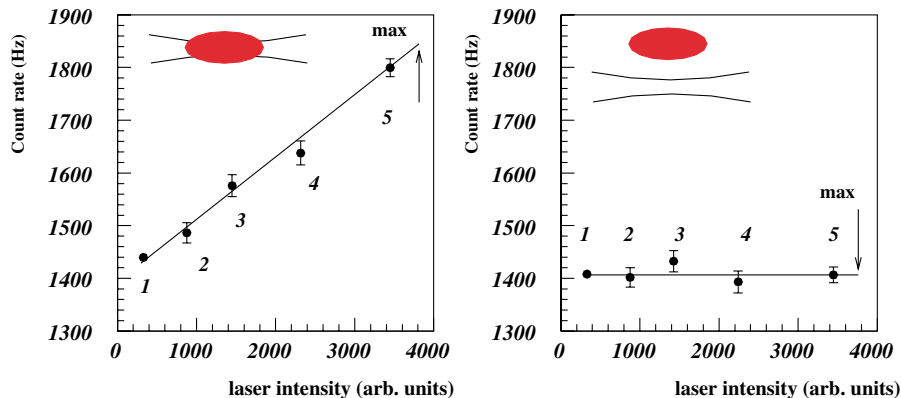


FIG. 7. (Color) Count rate versus the laser intensity. The laser wire was on (left) and off (right) the electron beam.

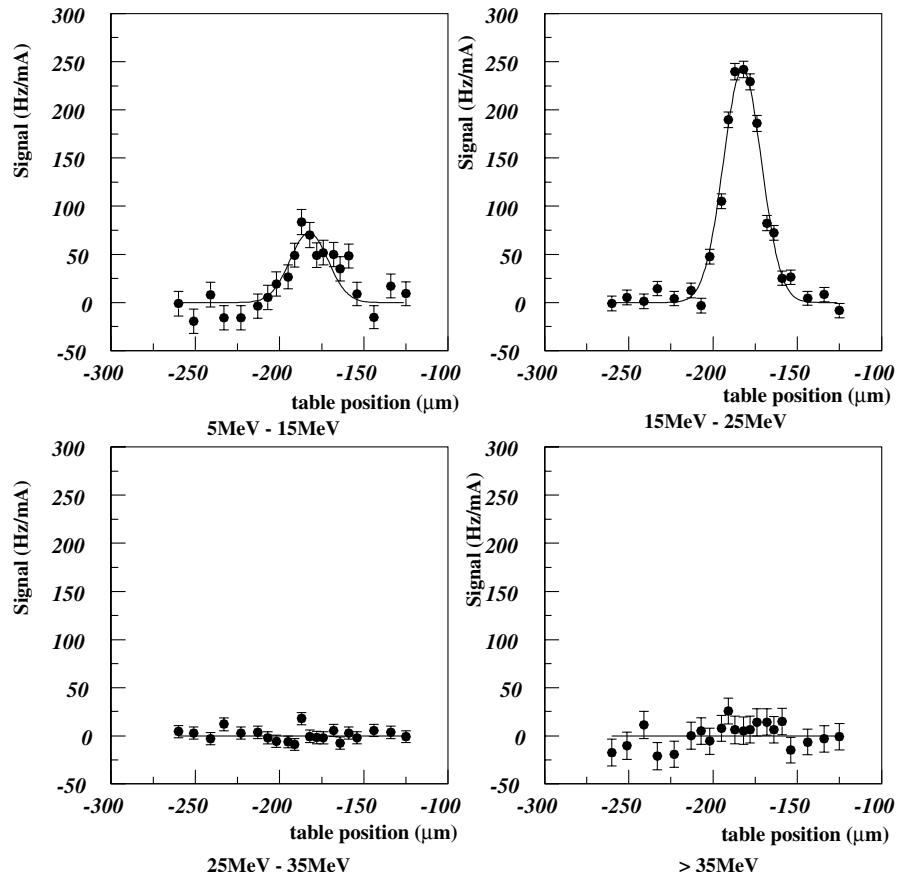


FIG. 8. Normalized signal count versus the laser wire position. The plots are for four different energy intervals (labeled by the subtitle at the bottom) of the same electron beam current (1.0–1.4 mA). Data from (2000/12/05).

Fig. 3. The arrows in Fig. 7 indicate the extrapolation. Finally, the signal count rate was defined by the difference between the maximum and the minimum count rates, where the minimum corresponds to the zero laser intensity.

(3) Then the signal count rate was normalized to the electron beam current. The resultant quantity is called a normalized signal rate (Hz/mA).

(4) Finally, we plotted the normalized signal rate as a function of the laser wire position. Procedure (2) was needed to prove linear increase of the obtained count rate with laser intensity and also to increase their statistical power. In order to check the goodness of the linear fit in procedure (2), the chi square (χ^2) per degree of freedom (ν) was calculated for each run. The resultant values, very close to $\chi^2/\nu = 1$, indicate goodness of the fit as well as the data.

2. Observed beam size σ_{obs} and its error

σ_{obs} was deduced from the signal count rates obtained above. In order to illustrate the analysis procedure, we take the data of 1.0–1.4 mA as an example. Figure 8

shows the signal rates as a function of the laser wire vertical positions for four energy bins. As expected, the Compton signals are mainly seen in the energy interval of 5–15 and 15–25 MeV. On the other hand, the signal rates above the Compton energy (>35 MeV) are consistent with zero. The chi square per degree of freedom that resulted from the zero-constant fitting for the data is found to be consistent with the statistical expectation.

After we confirmed that the Compton signals were seen only in the 5–25 MeV range for all the data (at any electron currents), we combined the data of 5–15 and 15–25 MeV regions. Then we fitted the data to a Gauss function with a center, width, and peak height being left as free parameters. Figure 9 shows the measured beam profiles obtained in this way for the (2000/12/5) data. The solid curves are resultant Gauss functions. Similar plots were made also for other data sets. We defined the beam size σ_{obs} by the width of the fitted Gauss functions. Table II lists our final results for σ_{obs} . As expected, the beam size for the 2nd data set (2000/12/07) is significantly larger than the other two. In the 2nd column, there are two errors listed for each σ_{obs} . Unparenthesized errors are those given by the Gauss fit while those in the

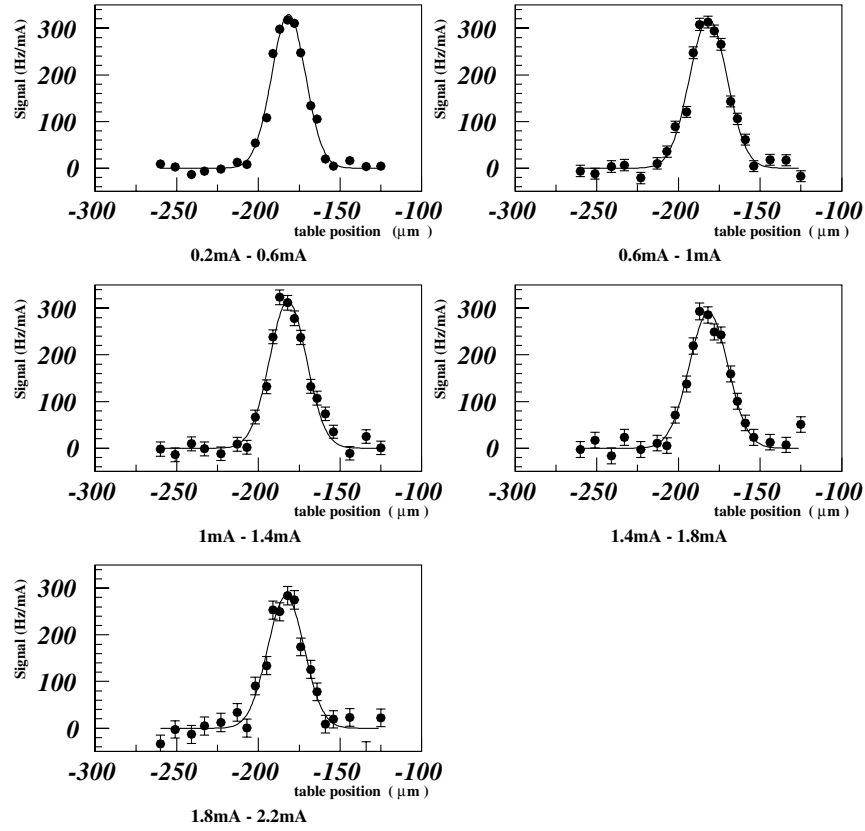


FIG. 9. Normalized signal count versus the laser wire position. The plots are the combined data of the energy interval 5–25 MeV for five different electron currents (labeled by the subtitle at the bottom) taken on (2000/12/05).

parentheses are obtained as follows. The 4th column is resultant χ^2/ν for the fits. We expect these χ^2 values would distribute around ν if they obey statistics. In reality, however, χ^2/ν 's are significantly larger than the unit,

indicating that there might be some systematic effects. They could be attributed to, for example, jitter and/or drift in the electron beam position. Since we have not identified their sources yet, we took a conservative way.

TABLE II. Summary of the electron beam size measurements.

Date	Current (mA)	Beam size σ_{obs} (μm)	χ^2/ν	σ_y (μm)	ϵ_y (10^{-11} m rad)
(2000/12/05)	0.4	10.38 ± 0.22 (± 0.35)	46.6/18	7.42 ± 0.56	0.95 ± 0.14
	0.8	11.51 ± 0.32 (± 0.47)	38.2/18	8.94 ± 0.65	1.38 ± 0.20
	1.2	11.34 ± 0.41 (± 0.53)	31.0/18	8.71 ± 0.73	1.31 ± 0.22
	1.6	11.93 ± 0.48 (± 0.55)	23.4/18	9.47 ± 0.72	1.55 ± 0.24
	2.0	11.23 ± 0.25 (± 0.72)	29.3/18	8.56 ± 0.97	1.27 ± 0.29
(2000/12/07)	1.2	24.91 ± 1.25 (± 1.25)	15.2/18	23.83 ± 1.31	10.05 ± 1.13
	1.6	21.65 ± 1.05 (± 1.51)	37.4/18	20.40 ± 1.60	7.36 ± 1.17
	2.0	21.45 ± 1.28 (± 1.53)	25.9/18	20.18 ± 1.63	7.21 ± 1.18
	2.4	23.07 ± 1.52 (± 2.33)	41.9/18	21.89 ± 2.46	8.48 ± 1.92
	2.8	23.80 ± 1.67 (± 2.17)	30.2/18	22.66 ± 2.29	9.09 ± 1.85
(2000/12/14)	1.2	10.65 ± 0.65 (± 0.96)	36.6/17	7.80 ± 1.34	1.53 ± 0.53
	1.6	9.09 ± 0.56 (± 0.63)	21.6/17	5.48 ± 1.11	0.76 ± 0.31
	2.0	9.22 ± 0.80 (± 0.94)	23.1/17	5.68 ± 1.56	0.81 ± 0.45
	2.4	9.47 ± 1.03 (± 1.14)	21.1/17	6.08 ± 1.81	0.93 ± 0.56
	2.8	11.48 ± 1.13 (± 1.14)	17.3/17	8.90 ± 1.49	1.99 ± 0.67

Namely, we enlarged uniformly all error bars so that resultant χ^2/ν 's became unit. New errors on σ_{obs} are listed in the parentheses in Table II. We employ these values in the rest of the analysis.

C. Measurement of the ATF damping ring parameters

Various ring parameters were monitored and/or measured during the experiment [10]. The methods and results of only relevant parameters will be briefly given. The β function at the laser wire position was measured as follows. First, by changing the strength of a quadrupole near the laser wire, we measured a change of the tune, namely, a change in the betatron oscillation with beam position monitors (BPMs). The change of the tune could be related to the β function as the quadrupole magnet varied. Actually we measured β functions at three quadrupole magnets. Then these β functions were used to predict the β function at the laser wire with a help of a ring's lattice model. The momentum spread σ_p/p was measured by a screen monitor at the extraction line, where the dispersion is very large [2]. η_x and η_y were also measured during the procedure of the dispersion correction. Because of poor resolution of the BPMs, we can set only the upper limit of these functions. The measured parameters in the damping ring are summarized in Table III. We notice that the β functions of (2000/12/05) and (2000/12/14) differ significantly.

D. Measurement of the beam waist

The beam waist w_0 was measured by two different methods both before and after the vertical emittance measurements [4]. One method was to measure the laser beam spot size $w(z)$ at far fields while the other was to utilize higher modes. The details of the measurement methods as well as their results are already reported [6]. We simply quote the results; the measurement confirmed that the results obtained with two different methods, before and after the experiment, are all consistent with each other. Thus we conclude that the beam waist re-

mained constant during the experiment, and the average value is given by $w_0 = 14.5 \pm 0.5 \mu\text{m}$.

IV. RESULTS AND DISCUSSIONS

First, we calculated the beam size σ_y from Eq. (1) using the measured laser beam waist w_0 . The results are listed in the 5th column of Table II. We notice that, from Table III, the term $\eta_y(\sigma_p/p)$ contributes less than $1.6 \mu\text{m}$, and that it can be neglected compared with σ_y of $\sim 10 \mu\text{m}$. Finally we use Eq. (2) to calculate ε_y ; the results are listed in the 6th column of Table II. In Fig. 10, the 1st and 3rd measurement results are plotted. We can draw several conclusions from this plot.

(1) The 1st and 3rd measurements agree well with each other in the common current interval.

(2) The ATF target value for the vertical emittance is $\varepsilon_y = 1.1 \times 10^{-11}$ mrad. This appears to be achieved; we will elaborate numerically on this point below.

(3) No clear dependence on the electron beam current was observed within our measurement errors.

To quantify the statement (2) above, we averaged these results in several ways. The averaged emittance in the common current interval (1.0–2.2 mA) is $(1.39 \pm 0.14) \times 10^{-11}$ mrad and $(0.92 \pm 0.23) \times 10^{-11}$ mrad, respectively, for the 1st and 3rd measurements. They agree fairly well with each other although they could be different because of the different ring conditions. The vertical emittance averaged over the entire current region is $(1.22 \pm 0.09) \times 10^{-11}$ mrad and $(1.02 \pm 0.20) \times 10^{-11}$ mrad, respectively, for the 1st and 3rd measurements. Strictly speaking, we cannot average the two values above since the measured current intervals as well as their ring conditions were different. However, encouraged by the agreement in the common current interval, and also to give a representative value for ε_y , we averaged them to obtain $(1.18 \pm 0.08) \times 10^{-11}$ mrad. This value should be interpreted as an upper limit of attainable emittance for 0.2–3.0 mA. This shows that the ATF damping ring has realized its design goal for

TABLE III. Summary of the parameters of the damping ring (measured value).

Parameter of DR	Sign	2000/12/05	2000/12/07	2000/12/14
Energy (GeV)	E_0		1.28	
Momentum spread	σ_p/p		$(8.0 - 5.5) \times 10^{-4}$	
rf voltage (kV)	V_{rf}		286	
rf frequency (MHz)	f_{rf}		714.005	
Momentum compaction	α_M		2.14×10^{-3}	
Tune	ν_x	15.18	15.18	15.15
	ν_y	8.58	8.58	8.51
β (m)	β_x	9.71 ± 0.07	9.73 ± 0.10	11.1 ± 0.08
at laser wire	β_y	5.77 ± 0.07	5.65 ± 0.14	3.97 ± 0.17
η (mm)	η_x		<10	
at laser wire	η_y		<2	

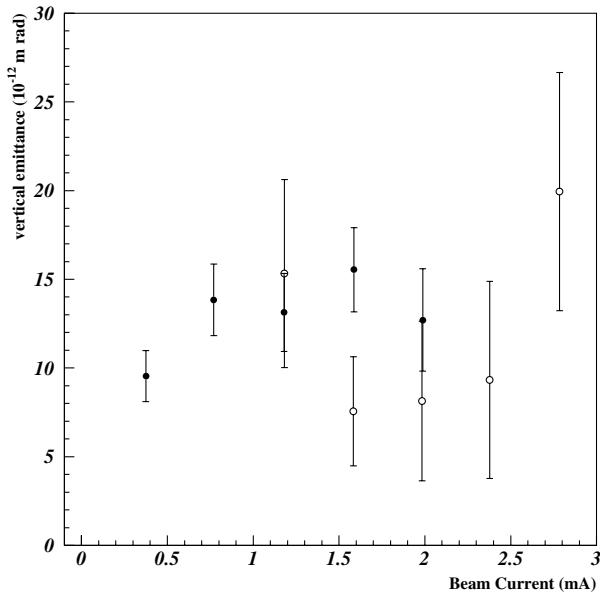


FIG. 10. Superposition of the two measurements. Solid and open circles represent, respectively, the results of (2000/12/05) and (2000/12/14).

the vertical emittance. These results are summarized in Table IV, which includes the 2nd measurement results for completeness. As anticipated, the 2nd measurement (2000/12/07) shows significantly bigger emittance than the other two.

In a low emittance ring such as ours, the vertical emittance is dominated by coupling with a much bigger horizontal emittance and/or residual vertical dispersion. The coupling in turn stems from skewed quadrupole components. In addition, other effects such as intrabeam scattering might be important. Effects due to intrabeam scattering have attracted much attention recently as the number of low emittance rings increases. Several theoretical studies have already been published [11–14]. The ATF damping ring is expected to offer the best place to study them experimentally. In fact, the effects due to the intrabeam scattering have been confirmed by several measurements at ATF; one is the Touschek lifetime of a

stored beam [15], another is the momentum spread, and the other is the horizontal emittance at the extraction line [2,16]. The vertical emittance is also expected to grow with a beam current due to the intrabeam scattering. For example, one model calculation [16] showed that the vertical emittance would increase by 40%–50% between the zero current and 3 mA. However, the accuracy of the present measurements is not sufficient to prove or disprove it. This important phenomenon awaits further investigation from both theoretical and experimental sides [17].

V. CONCLUSION

In this paper, we have described vertical emittance measurements of the ATF damping ring with the laser wire beam profile monitor. This monitor was installed at the north straight section of the ATF damping ring. We carried out emittance measurements 3 times with different ring conditions. Although we have not described in detail, the observed signals were unambiguously identified as the Compton photons; the counting rate as well as its energy spectrum agreed well with their expected value and shape [10]. When the ring optics was tuned for a low emittance, it was confirmed that the vertical emittance of $\varepsilon_y = (1.18 \pm 0.08) \times 10^{-11}$ mrad was achieved. This value shows that the ATF damping ring has realized its target emittance also vertically.

ACKNOWLEDGMENTS

We would like to express our gratitude to all members of the ATF group for their helpful support. We are also grateful to Dr. M. Ross, Dr. J. Frisch, and Dr. T. Kotseroglou for their useful discussions with our laser wire experiment. It is our pleasure to thank Professor H. Sugawara, Professor M. Kihara, Professor Y. Kimura, Professor S. Iwata, and Professor K. Takata for their support and encouragement. This research was partially supported by Grant-in-Aid Scientific Research (1344078) from the Ministry of Education, Science, Sports and Culture of Japan.

TABLE IV. Summary of the vertical emittance measurements.

Measurement date	ε_y (10^{-11} mrad)	Electron beam Current (mA)
2000/12/05	1.22 ± 0.09 (*)	0.2–2.2
	1.39 ± 0.14	1.0–2.2
2000/12/07	8.37 ± 0.60	1.0–3.0
	8.26 ± 0.67	1.0–2.2
2000/12/14	1.02 ± 0.20 (**)	1.0–3.0
	0.92 ± 0.23	1.0–2.2
Average of (*) and (**)	1.18 ± 0.08	

*Present address: High Energy Accelerator Research Organization (KEK), Ibaraki, Japan.

†Corresponding author.

Email address: sasao@scphys.kyoto-u.ac.jp

‡Present address: National Institute of Radiological Sciences (NIRS), Chiba, Japan.

- [1] F. Hinode, S. Kawabata, H. Matsumoto, K. Oide, K. Takata, S. Takeda, and J. Urakawa, KEK Internal Report No. 95-4, 1995.
- [2] T. Okugi, T. Hirose, H. Hayano, S. Kamada, K. Kubo, T. Naito, K. Oide, K. Takata, S. Takeda, N. Terunuma, N. Toge, J. Urakawa, S. Kashiwagi, M. Takano, D. McCormick, M. Minty, M. Ross, M. Woodley,

- F. Zimmermann, and J. Corlett, *Phys. Rev. ST Accel. Beams* **2**, 022801 (1999)
- [3] Y. Takayama, T. Okugi, T. Miyahara, S. Kamada, J. Urakawa, and T. Naito, in *Proceedings of the 1999 Particle Accelerator Conference, New York* (IEEE, Piscataway, NJ, 1999).
- [4] H. Sakai, N. Sasao, S. Araki, Y. Higashi, T. Okugi, T. Taniguchi, J. Urakawa, and M. Takano, *Nucl. Instrum. Methods Phys. Res., Sect. A* **455**, 113–117 (2000).
- [5] H. Sakai, Y. Honda, N. Sasao, S. Araki, Y. Higashi, T. Okugi, T. Taniguchi, J. Urakawa, and M. Takano, *Phys. Rev. ST Accel. Beams* **4**, 022801 (2001).
- [6] H. Sakai, Y. Honda, N. Sasao, S. Araki, Y. Higashi, T. Okugi, T. Taniguchi, J. Urakawa, and M. Takano, *Jpn. J. Appl. Phys.* **41**, 6398–6408 (2002).
- [7] There is no direct measurement confirming this value. However, judging from energy spread measurements as a function of the stored time, the beam was found to be in equilibrium at least about 0.2 sec after the injection.
- [8] The background events stem both from scattering of the beam electrons by residual gas molecules and intrabeam scattering in a bunch. Stray electrons created by the processes in turn produce high energy photons whose spectrum extends up to a few tens of MeV.
- [9] K. Kubo, in *Proceedings of the 6th European Particle Accelerator Conference, Stockholm, 1998* (IOP, Bristol, U.K., 1998).
- [10] H. Sakai, Ph.D. thesis, Kyoto University, 2001.
- [11] J. Le Duff, *Nucl. Instrum. Methods Phys. Res., Sect. A* **239**, 83 (1985).
- [12] J. D. Bjorken and S. K. Mtingwa, *Part. Accel.* **13**, 115 (1983).
- [13] A. Pwinski, DESY Report No. 90-113, 1990.
- [14] K. Kubo and K. Oide, *Phys. Rev. ST Accel. Beams* **4**, 124401 (2001).
- [15] T. Okugi, H. Hayano, K. Kubo, T. Naito, N. Terunuma, J. Urakawa, T. Hirose, F. Zimmermann, and T. O. Raubenheimer, *Nucl. Instrum. Methods Phys. Res., Sect. A* **455**, 207–212 (2000).
- [16] K. Kubo *et al.*, *Phys. Rev. Lett.* **88**, 194801 (2002).
- [17] K. L. Bane *et al.*, in *Proceedings of the 2001 Particle Accelerator Conference, Chicago* (IEEE, Piscataway, NJ, 2001).